

## Numerical approach for tailoring performance of magnetoelectric PZT/terfenol-D laminated composites

Jimmy. H. Wang, Shashank Priya, Ruyan Guo, and Amar S. Bhalla

Citation: *Journal of Applied Physics* **107**, 084110 (2010); doi: 10.1063/1.3387815

View online: <http://dx.doi.org/10.1063/1.3387815>

View Table of Contents: <http://scitation.aip.org/content/aip/journal/jap/107/8?ver=pdfcov>

Published by the [AIP Publishing](#)

---

### Articles you may be interested in

[The effect of field-orientation on the magnetoelectric coupling in Terfenol-D/PZT/Terfenol-D laminated structure](#)  
J. Appl. Phys. **116**, 173910 (2014); 10.1063/1.4901069

[The influence of low-level pre-stressing on resonant magnetoelectric coupling in Terfenol-D/PZT/Terfenol-D laminated composite structure](#)  
J. Appl. Phys. **115**, 193906 (2014); 10.1063/1.4876721

[A uniform model for direct and converse magnetoelectric effect in laminated composite](#)  
Appl. Phys. Lett. **104**, 202904 (2014); 10.1063/1.4878559

[Magnetodielectric effect and electric-induced magnetic permeability in magnetoelectric laminate composite under low inspiring signal](#)  
J. Appl. Phys. **113**, 043907 (2013); 10.1063/1.4780828

[Giant magnetodielectric effect in Terfenol-D/PZT magnetoelectric laminate composite](#)  
J. Appl. Phys. **110**, 014508 (2011); 10.1063/1.3603042

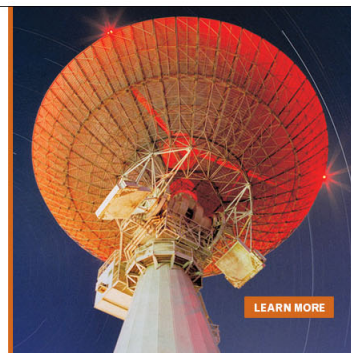
---

MIT LINCOLN  
LABORATORY  
CAREERS

Discover the satisfaction of  
innovation and service  
to the nation

- Space Control
- Air & Missile Defense
- Communications Systems & Cyber Security
- Intelligence, Surveillance and Reconnaissance Systems
- Advanced Electronics
- Tactical Systems
- Homeland Protection
- Air Traffic Control

 **LINCOLN LABORATORY**  
MASSACHUSETTS INSTITUTE OF TECHNOLOGY



# Numerical approach for tailoring performance of magnetoelectric PZT/terfenol-D laminated composites

Jimmy. H. Wang,<sup>1,a)</sup> Shashank Priya,<sup>2</sup> Ruyan Guo,<sup>1</sup> and Amar S. Bhalla<sup>1</sup>

<sup>1</sup>Department of Electrical and Computer Engineering, MeMDRL, University of Texas at San Antonio, San Antonio, Texas 78249, USA

<sup>2</sup>Department of Materials Science and Engineering, CEHMS, Virginia Polytechnic Institute and State University, Blacksburg, Virginia 24061, USA

(Received 9 February 2010; accepted 8 March 2010; published online 27 April 2010)

Rising demands in design of metamaterials requires better understanding of coupling phenomena in composite systems. Materials exhibiting product properties have effective magnitude of physical constants surpassing those of naturally existing materials. In this manuscript, we conduct numerical modeling of laminated terfenol-D/PZT/terfenol-D magnetoelectric composites with sandwich structure coupled through elastic interactions across the bonding layer. Developed magnetoelectric model couples the piezoelectric and magnetostriction constitutive equations with Langevin theory for simulating the saturated elastic response in composites. Simulated results were found to be in good agreement with the experimental results. Based upon the developed model we predict 17% improvement of magnetoelectric coefficient for sandwich structure through proper rotation of polarization in individual layers. © 2010 American Institute of Physics. [doi:10.1063/1.3387815]

## I. INTRODUCTION

Single phase magnetoelectric (ME) materials exhibit limited magnitude of ME coefficient due to low permittivity and permeability ( $< \sqrt{\epsilon_{ii}\mu_{jj}^p}$ ).<sup>1</sup> Not only the reported single phase ME materials have weak ME coefficients but they exhibit ME effect far below room temperature.<sup>2-5</sup> Composites based on product properties can provide enhanced ME coefficient by selecting proper materials, connectivity, and poling direction. Ferroelectric-ferrimagnetic combinations based upon Pb(Zr,Ti)O<sub>3</sub> (PZT) and ferrites and PZT-TbDyFe<sub>2</sub> (terfenol-D) combinations have emerged as the leading candidates in this aspect. Recently, laminated structure with PZT fibers embedded in Metglas foils have been shown to provide giant performance due to its inherent flexibility and high permeability of amorphous phase. A list of several reported ME materials and composite geometries were presented by Ryu *et al.*<sup>6</sup> and recently by Priya *et al.*<sup>7</sup> A giant ME effect has reported in the laminated structures of piezoelectrics (Pb(Mg,Nb)O<sub>3</sub>-PbTiO<sub>3</sub> (PMN-PT) single crystal, PMN-PT ceramic, and PZT) and magnetostrictive terfenol-D at dc bias of 4 kOe and frequency of 1 kHz. The ME voltage coefficient was as high as  $\sim 5000$  mV/cm Oe, which is almost two orders of magnitude higher than the reported values for sintered composites. In this manuscript, we utilize the experimental results reported in Ref. 6 and develop numerical model to fit the results and further modify the model to predict the conditions improved performance.

## II. MODEL AND SYSTEM GEOMETRY

Figure 1(a) shows the modeling geometry of laminated ME device having a diameter of 12.7 mm. The system is in disk shape consisting of three layers. A piezoelectric layer,

PZT, with thicknesses of 0.5, 0.6, or 0.7 mm is sandwiched in between magnetostrictive terfenol-D with thickness of 1 mm. The parameters used in the model for PZT and terfenol-D are listed in Table I. Piezoelectric voltage coefficient  $e_{31}$  of PZT was estimated to be one-third of  $e_{33}$  with negative sign based upon the reason that most PZTs have Poisson's ratio around 0.3. Magnetostriction ( $N$ ) matrix was calculated from the saturation strains and by using the expression derived by Newnham<sup>8</sup> given as follows:  $N_{11} = (8\lambda_{100})/I_s^2$ ,  $N_{12} = -(8\lambda_{100})/(3I_s^2)$ , and  $N_{44} = (3\lambda_{111})/I_s^2$ , assuming terfenol-D has pseudocubic structure. In the magnetic/electric transformation process, there are three major losses as follows: electrical, magnetic, and mechanical losses. Due to lack of information on all these three different quantities, only dielectric loss [ $\tan(\delta)$ ] was considered in the model. The effect of bonding material layers was neglected considering that the laminated composites were assembled in ideal condition. The density for PZT was taken to be 8000 kg/m<sup>3</sup> and that for terfenol-D it was estimated to be 9200 kg/m<sup>3</sup> from values reported by Sandlund *et al.*<sup>9</sup>

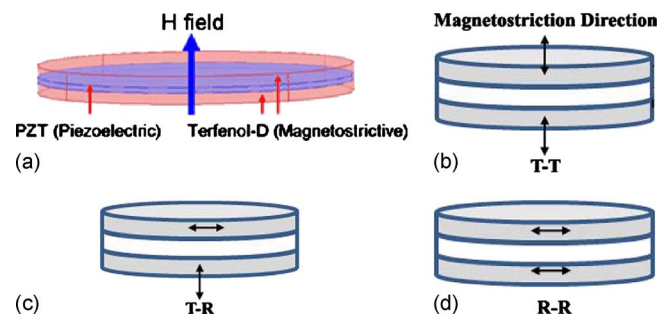


FIG. 1. (Color online) (a) Geometry of laminated magnetoelectric/piezoelectric/magnetostriction structure where piezoelectric PZT disk is sandwiched between two magnetostrictive terfenol-D disk, (b) T-T composite, (c) T-R composite, and (d) R-R composite.

<sup>a)</sup>Electronic mail: hsiaoyuan.wang@utsa.edu.

TABLE I. Material properties of PZT and terfenol-D used in the model.

PZT (APC840)			Terfenol-D		
$E$	1250	$\mu$	5	$\lambda_{111}$	$1.7 \times 10^{-3}$
$\tan \delta$	0.004	$N_{11}$ (m <sup>2</sup> /A <sup>2</sup> )	$2.58 \times 10^{-9}$ <sup>a</sup>	$\lambda_{100}$	$0.1 \times 10^{-3}$
$e_{33}$ (mV/m/N)	25.6	$N_{12}$ (m <sup>2</sup> /A <sup>2</sup> )	$8.6 \times 10^{-10}$ <sup>a</sup>		
$d_{33}$ (pC/N)	320	$N_{44}$ (m <sup>2</sup> /A <sup>2</sup> )	$1.64 \times 10^{-8}$ <sup>a</sup>		
$C_{11}$ (GPa)	130	$C_{11}$ (GPa)	82		
$C_{12}$ (GPa)	80	$C_{12}$ (GPa)	40		
$C_{44}$ (GPa)	23	$C_{44}$ (GPa)	38		

<sup>a</sup> $N_{ij}$ s are calculated based on the measurement values  $\lambda_{111}$  and  $\lambda_{100}$ .

Three different configurations of laminated ME composites were analyzed as shown in Fig. 1(b). PZTs in all three configurations were oriented along thickness direction (z-direction in the simulation model). In Fig. 1(b), the composite was fabricated by using two terfenol-D disks that were oriented along the thickness direction (T-T composite represents the two magnetostrictive domains oriented in thickness direction). In Fig. 1(c), the composite was fabricated with one terfenol-D disk oriented along the thickness direction and the other terfenol-D disk along the radial direction (T-R composite). In Fig. 1(d), the composite was fabricated from two disks that have orientation along the radial direction (R-R composite). Experimentally, it was shown that R-R composite exhibits the highest ME voltage coefficient.

The ME model was constructed by coupling piezoelectric and magnetostriction constitutive equations given as

$$D_i = e_{imn}X_{mn} + \varepsilon_{ij}E_j, \quad (1)$$

$$X_{ij} = c_{ijmn}x_{mn} - e_{mij}E_m, \quad (2)$$

where  $D$  is the dielectric displacement,  $e$  the piezovoltage coefficient,  $X$  the stress,  $\varepsilon$  the permittivity,  $E$  the electric field,  $c$  the elastic stiffness, and  $x$  the strain. Detailed description of piezoelectric model and its verification has been reported elsewhere.<sup>10</sup>

Magnetostrictive materials are characterized by the state variables  $u$ ,  $v$ ,  $w$ , and  $H$ , where  $u$ ,  $v$ , and  $w$  are material displacements in spatial coordinates. Here, the magnetic field  $H$  was used instead of magnetization,  $I$ . The constitutive equations for magnetostriction model are

$$B_i = \mu_{ij}H_j + N_{ijkl}x_{kl}H_j, \quad (3)$$

$$X_{ij} = c_{ijkl}x_{kl} - N_{klij}H_kH_l, \quad (4)$$

where  $B_i$  is the magnetic displacement,  $\mu_{ij}$  the permeability,  $x_{kl}$  the strain,  $X_{ij}$  the stress,  $N_{ijkl}$  the magnetostrictive coefficient, and  $c_{ijkl}$  the elastic stiffness. The energy of composite system is a combination of electrical, magnetic and elastic energy given as

$$W_E = \frac{1}{2}(D_iE_i), \quad (5)$$

$$W_M = \frac{1}{2}(H_iB_i), \quad (6)$$

$$W_S = \frac{1}{2}(X_{ij}x_{ij}), \quad (7)$$

$$W_{\text{total}} = W_S + W_M - W_E. \quad (8)$$

where  $W_E$  is the electrical energy,  $W_M$  is the magnetic energy,  $W_S$  is the elastic energy, and  $W_{\text{total}}$  the total energy of the system. The term  $N_{ijkl}x_{kl}H_j$  in Eq. (3) is inverse magnetostrictive effect and  $N_{klij}H_kH_l$  in Eq. (4) is the magnetostriction effect. Above equations can be readily obtained from free energy derivations under constant temperature. The negative sign of  $W_E$  from Eq. (8) comes from the definition that  $E = -\nabla V$ .

### III. SIMULATION RESULTS AND DISCUSSIONS

Initially, R-R configuration was selected for simulation as it has been reported to exhibit the highest ME coefficient among three different configurations shown in Fig. 1. In our models, (111) direction of terfenol-D was aligned along the X axis of system. Simulated results along with experimentally measured ME voltage coefficients as a function of bias magnetic field are shown in Fig. 2(a). In order to prevent nonconvergent simulations, the center point of the bottom terfenol disk was constrained and one of the bottom edge point was constrained in z-direction. The ME voltage coefficient ( $dE/dH$ ) was computed by changing the magnetic bias field from 100 to 5000 Oe and a coupling ac field of 2 Oe along thickness direction. The ac field was simulated by considering one cycle of additional  $\pm\sqrt{2}$  Oe bias along thickness direction. PZT thickness of 0.5, 0.6, and 0.7 mm were examined in the simulations and computed results are compared with experimental results. Simulated behavior of laminate composite follows similar trend as the reported experimental data below magnetic bias of 1000 Oe. Discrepancy between the simulated and experimental results was found to occur above the magnetic bias of 1000 Oe as shown in Fig. 2(a). In this set of simulations the magnetostriction effect exhibited quadratic behavior in magnetomechanical response [by using Eq. (2)] while the piezoelectric coefficient exhibited linear behavior in electromechanical response. Therefore, both experimental and simulated results exhibited non-linear variation at low magnetic field ( $\sim 500$  Oe). Above 1000 Oe, the simulated ME coefficients did not reach saturation as the theoretical model did not include saturation ef-

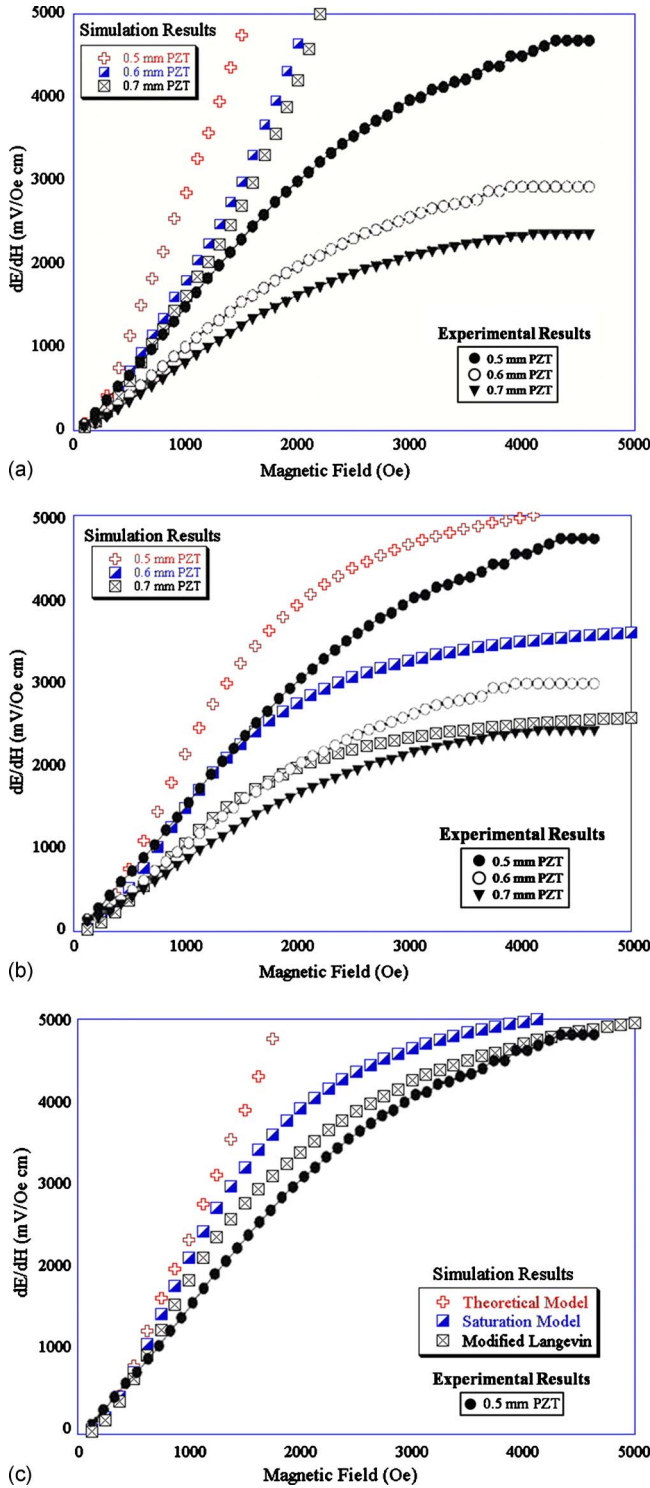


FIG. 2. (Color online) Plots of magnetic bias field vs ME voltage coefficient for R-R composites (a) experimental results and theoretical model (b) experimental results and modified saturation model (c) comparison of theoretical, modified saturation, and Langevin model with the experimental results.

fects. In order to overcome the saturation effect, further modifications were made in the model.

Both piezoelectric and magnetostrictive materials show saturated strains proportional to the maximum electrical or magnetic polarization achievable under a given set of boundary conditions which can be included in the constitutive equations as

$$X_{ij} = c_{ijmn}x_{mn} - e_{mij} \times \frac{E_m}{\frac{E_m}{E_s} + 1}, \quad (9)$$

$$X_{ij} = c_{ijkl}x_{kl} - N_{klij} \frac{H_k H_l}{\frac{H_k H_l}{H_s^2} + 1}. \quad (10)$$

Equation (9) shows that strain-charge relationship follows linear trend when the applied electric field is small compared to the saturated field. At large field, the right term of Eq. (9) approaches a limit approximately given as  $e_{mij}E_s$ . A similar approach was used for the magnetostrictive model with double  $H$  fields as shown in Eq. (10). Both modified equations preserve their tensor behaviors at low electric or magnetic fields. The combination of Eqs. (9) and (10) is referred as saturation model, which will be used in the discussions below.

The ME voltage coefficient was evaluated using the modified constitutive equations and the results are compared with the experimental data as shown in Fig. 2(b). Experimentally, the maximum ME voltage coefficient of  $\sim 4600$  mV/Oe cm was obtained at magnetic bias of  $\sim 4500$  Oe while in simulation the maximum ME value of 5200 mV/Oe cm was found at 5000 Oe. Owing to the assumption of perfect interfacial boundaries between PZT and terfenol-D, the simulation values show minor difference with the experimental data.

It is known that in magnetostrictive materials the origin of saturation strain is from saturation of magnetization. Langevin function<sup>11</sup> is widely utilized for calculation of magnetization of an ideal paramagnetic material. In paramagnetic phase, the magnetization and magnetic field can be related as

$$I(x) = C \left( \coth x - \frac{1}{x} \right), \quad (11)$$

$$x = \frac{H \times I_0}{k_B T},$$

where  $I(x)$  is the magnetization,  $C$  is a materials variable,  $I_0$  is the demagnetization state,  $k_B$  and  $T$  are the Boltzmann constant and temperature. Since terfenol-D has high symmetry (cubic or pseudocubic crystal structure), its third rank hysteresis behavior can be ignored and the modified Langevin equation can be written as

$$X_{ij} = c_{ijkl}x_{kl} - N_{klij}H'_k H'_l, \quad (12)$$

$$H'_k = C \left[ \coth(BH_k) - \frac{1}{BH_k} \right],$$

where  $H'_k$  and  $H'_l$  are the effective magnetizations,  $H_k$  is the applied magnetic field,  $C$  and  $B$  are coefficients obtained by curve fitting and were estimated to be  $C=251$  A/m and  $B=8.4 \times 10^{-6}$  m/A (estimated by fitting  $\lambda_{100}$  curve). In order to verify the magnitude of constants, a simulation run was performed on  $\lambda_{111}$  and results were found to be in good



agreement with the experimental results. Next, modeling of the ME coefficient was performed with R-R configuration as described in Figs. 2(a) and 2(b). Results from three different simulation models are plotted in Fig. 2(c), where PZT layer had a thickness of 5 nm. From this figure, it can be seen that at low magnetic bias the saturation model overestimates the ME voltage coefficient, while in high magnetic bias region the modeled ME voltage coefficient saturates more rapidly as compared to that of modified Langevin model and experimental results. It was also found that simulated ME voltage

coefficients from modified Langevin model are in close agreement to experimental results where ME voltage coefficient reaches magnitude of 4950 mV/Oe cm at magnetic bias of 5000 Oe.

Next we try to address the question “why R-R composite exhibits the best performance?” In order to evaluate the magnetostrictive coefficient  $N$  in any arbitrary direction, the matrix form  $N_{ij}$  is more useful for calculations as compared to the tensor form  $N_{mnop}$ . A  $6 \times 6$  matrix,  $\alpha$ , is commonly used for transformation of a fourth rank matrix and is defined as

$$\alpha = \begin{pmatrix} a_{11}^2 & a_{12}^2 & a_{13}^2 & 2a_{12}a_{13} & 2a_{11}a_{13} & 2a_{11}a_{12} \\ a_{21}^2 & a_{22}^2 & a_{23}^2 & 2a_{22}a_{23} & 2a_{21}a_{23} & 2a_{21}a_{22} \\ a_{31}^2 & a_{32}^2 & a_{33}^2 & 2a_{32}a_{33} & 2a_{31}a_{33} & 2a_{31}a_{32} \\ 2a_{21}a_{31} & 2a_{22}a_{32} & 2a_{23}a_{33} & a_{23}a_{32} + a_{22}a_{33} & a_{23}a_{31} + a_{21}a_{33} & a_{22}a_{31} + a_{21}a_{32} \\ 2a_{11}a_{31} & 2a_{12}a_{32} & 2a_{13}a_{33} & a_{13}a_{32} + a_{12}a_{33} & a_{13}a_{31} + a_{11}a_{33} & a_{12}a_{31} + a_{11}a_{32} \\ 2a_{11}a_{21} & 2a_{12}a_{22} & 2a_{13}a_{23} & a_{13}a_{22} + a_{12}a_{23} & a_{13}a_{21} + a_{11}a_{23} & a_{12}a_{21} + a_{11}a_{22} \end{pmatrix}, \quad (13)$$

where  $a_{ij}$  is a  $3 \times 3$  matrix used for direction transformation between cartesian and spherical coordinates, given by Eq. (10) and Fig. 3:

$$a_{ij} = \begin{pmatrix} \sin \theta \cos \phi & \sin \theta \sin \phi & \cos \theta \\ \cos \theta \cos \phi & \cos \theta \sin \phi & -\sin \theta \\ -\sin \phi & \cos \phi & 0 \end{pmatrix}, \quad (14)$$

where  $\theta$  is the angle between rotated direction and crystallographic  $Z_3$  axis, while  $\phi$  is the angle between projection of rotated direction on  $Z_1$ - $Z_2$  plane and  $Z_1$  axis. The magnetostrictive coefficient  $N'_{ij}$  in arbitrary direction can be evaluated through matrix transformation as

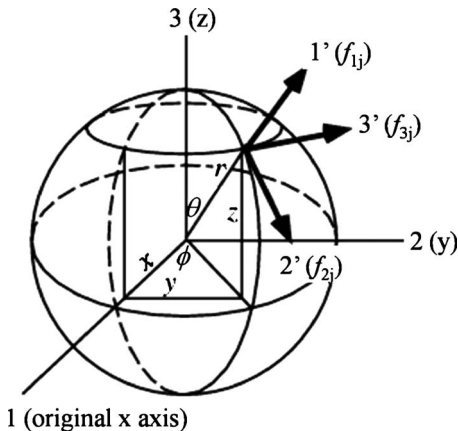


FIG. 3. (Color online) Relationship of directions/angles between cartesian coordinates and spherical coordinates.  $1'$  corresponds to the direct response.  $2'$  and  $3'$  directions are perpendicular to each other at the same time perpendicular to  $1'$  (in tensor transformations of  $f_{2j}$  and  $f_{3j}$ ).

$$N'_{ij} = \alpha N \alpha_t, \quad (15)$$

where  $\alpha_t$  is transpose of  $\alpha$  matrix. The parametric plot of direct response  $N'_{11}$  can be calculated based on Eq. (15) as

$$N'_{11} = a_{11}^2(a_{12}^2N_{12} + a_{13}^2N_{12} + a_{11}^2N_{11}) + a_{12}^2(a_{11}^2N_{12} + a_{13}^2N_{12} + a_{12}^2N_{11}) + a_{13}^2(a_{11}^2N_{12} + a_{12}^2N_{12} + a_{13}^2N_{11}) + 4a_{11}^2a_{12}^2N_{44} + 4a_{11}^2a_{13}^2N_{44} + 4a_{12}^2a_{13}^2N_{44}. \quad (16)$$

Figure 4(a) shows the contour of magnetostrictive coefficient  $N'_{11}$  for terfenol-D in arbitrary directions. The coefficient  $N'_{11}$  represents the magnitude of magnetostriction along the direction of applied magnetic field. The maximum direct magnetostrictive response of terfenol-D occurs when the magnetic field is aligned along  $\langle 111 \rangle$  axis.

It is interesting to note that the ME coefficient of specific composite structure can also be improved by rotating the samples along optimum crystallographic direction. The ME coefficient of R-R configuration depends on the magnitude of compressive stress exerted by the magnetostrictive material on piezoelectric, i.e., the effective  $N_{\perp}$  values of magnetostrictive materials. Here,  $N_{\perp}$  is defined as the resulting transverse mechanical response perpendicular to the applied magnetic field. In spherical coordinates, the transverse response is estimated from combination of two quantities  $N'_{12}$  and  $N'_{13}$ . The prime notation in  $N'_{12}$  and  $N'_{13}$  is used to avoid the confusion with crystallographic  $N_{12}$  and  $N_{13}$  coefficients respectively. The coefficients  $N'_{12}$  and  $N'_{13}$  can be calculated in arbitrary direction by using Eqs. (13)–(15) as

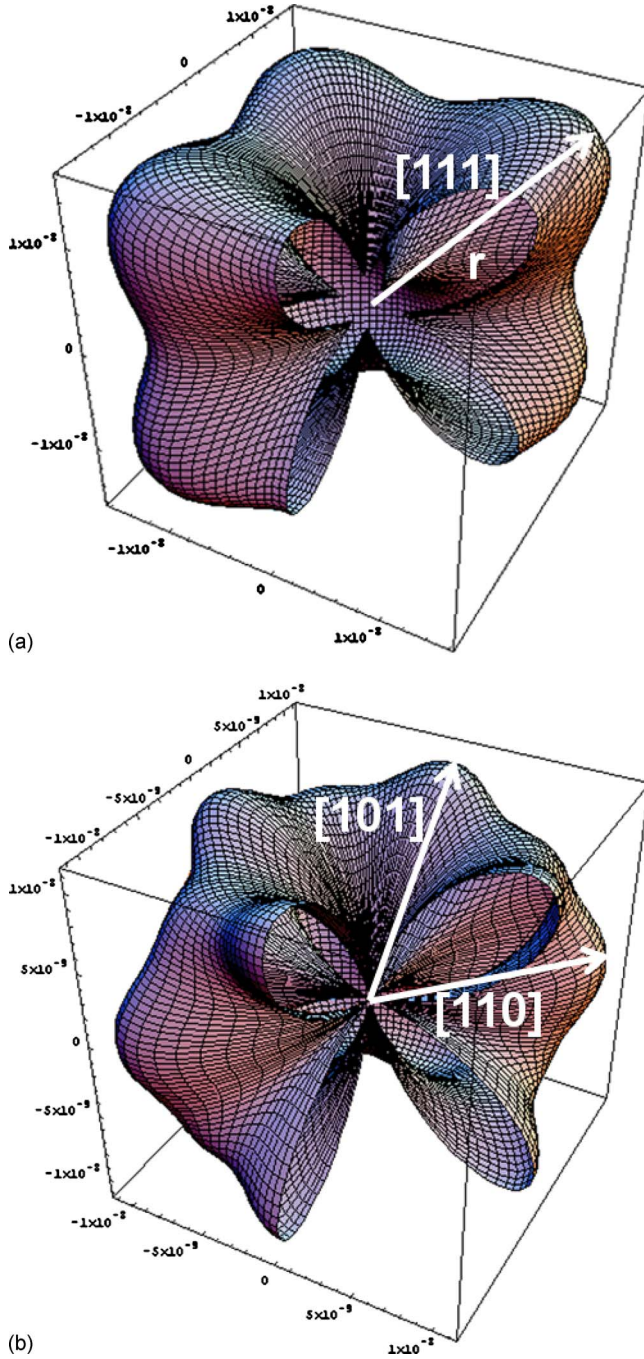


FIG. 4. (Color online) Contour of effective magnetostrictive coefficient of terfenol-D (a) direct response  $N'_{11}$ . The maximum direct magnetostrictive response occurs when the field is aligned along one of the  $\langle 111 \rangle$  directions (b) transversal response  $N_{\perp}$  of terfenol-D. The maximum transversal response occurs along  $\langle 110 \rangle$  directions.

$$\begin{aligned}
 N'_{12} = & (a_{12}^2 a_{21}^2 + a_{13}^2 a_{21}^2 + a_{11}^2 a_{22}^2 + a_{13}^2 a_{22}^2 + a_{11}^2 a_{23}^2 \\
 & + a_{12}^2 a_{23}^2) N_{12} + (a_{11}^2 a_{21}^2 + a_{12}^2 a_{22}^2 + a_{13}^2 a_{23}^2) N_{11} \\
 & + 4a_{11} a_{12} a_{21} a_{22} N_{44} + 4a_{11} a_{13} a_{21} a_{23} N_{44} \\
 & + 4a_{12} a_{13} a_{22} a_{23} N_{44},
 \end{aligned} \quad (17)$$

$$\begin{aligned}
 N'_{13} = & (a_{12}^2 a_{31}^2 + a_{13}^2 a_{31}^2 + a_{11}^2 a_{32}^2 + a_{13}^2 a_{32}^2 + a_{11}^2 a_{33}^2 \\
 & + a_{12}^2 a_{33}^2) N_{12} + (a_{11}^2 a_{31}^2 + a_{12}^2 a_{32}^2 + a_{13}^2 a_{33}^2) N_{11} \\
 & + a_{11} a_{12} a_{31} a_{32} N_{44} + 4a_{11} a_{13} a_{31} a_{33} N_{44}
 \end{aligned}$$

$$+ 4a_{12} a_{13} a_{32} a_{33} N_{44}. \quad (18)$$

Since  $N'_{12}$  and  $N'_{13}$  are always perpendicular to each other, the transversal magnetostrictive response  $N_{\perp}$  can be calculated by combining the coefficients  $N'_{12}$  and  $N'_{13}$  as

$$N_{\perp} = \sqrt{N_{12}'^2 + N_{13}'^2}. \quad (19)$$

The contour of effective transversal magnetostrictive coefficient  $N_{\perp}$  in various directions is plotted in Fig. 4(b). It can be observed from this figure that the maximum  $N_{\perp}$  occurs when the magnetic field is applied along the  $\langle 110 \rangle$  crystallographic directions of terfenol-D where the cosine angle between  $\langle 110 \rangle$  and  $Z_3$  axis is approximately  $45^\circ$ . Experimentally the best results were found when terfenol-D was oriented along  $\langle 111 \rangle$  where the cosine angle between  $\langle 111 \rangle$  and  $Z_3$  axis is approximately  $57^\circ$  ( $\cos \theta = 1/\sqrt{3}$ ). The calculation shown here indicates that ME coefficient can be improved by aligning  $\langle 110 \rangle$  axis of terfenol-D with applied field direction.

In order to evaluate the transversal force applied to the PZT, the mean transversal stress of each terfenol-D disk was estimated through crystal rotations from thickness direction along  $(001)$  to  $(111)$  to  $(110)$  as shown in Fig. 5(a). In this set of simulation, 5000 Oe bias and  $\pm 2$  Oe ac field was applied. Figure 5(b) shows the mean transversal stress corresponding to the crystal rotation. The mean transversal stress was estimated by integrating the transversal stresses over the disk surface by using Eq. (12) and averaging over unit area. From Fig. 5(b) there are two local maximum of average transversal stress, one around  $16^\circ$  and the other along  $(111)$  direction. The maximum mean transversal stress obtained at  $(110)$  was approximately 380 MPa. Notice that unlike the case of  $(001)$  and  $(111)$ , when thickness direction was aligned at crystallographic  $(110)$  direction, the resulting stress on the surface is not uniform along radial direction. This indicates further improvement in ME coupling could be possible by engineering the geometry of the system, possibly elliptical disk.

The disk shape PZT was then sandwiched by magnetic layers of terfenol-D having its  $\langle 110 \rangle$  crystallographic axis along the applied magnetic field direction ( $z$ -direction). Figure 6 shows the simulation of ME voltage coefficient with respect to applied magnetic bias for this scenario. The simulation results show an approximately 17% improvement of ME effect by using this configuration where the magnitude of ME voltage coefficient reaches  $\sim 5800$  mV/Oe cm at magnetic field of 5000 Oe.

#### IV. CONCLUSION

The ME voltage coefficient simulated using the modified Langevin model was found to provide the best fit for reported experimental results. Effective direct magnetostrictive response  $N'_{11}$  was calculated over the three-dimensional space and the maximum in  $N'_{11}$  occurred along the  $\langle 111 \rangle$  crystallographic direction. Effective transversal magnetostrictive coefficient  $N_{\perp}$  showed the maximum response when magnetic field was applied along  $\langle 110 \rangle$  crystallographic direction of terfenol-D. Based on this study, it is suggested that

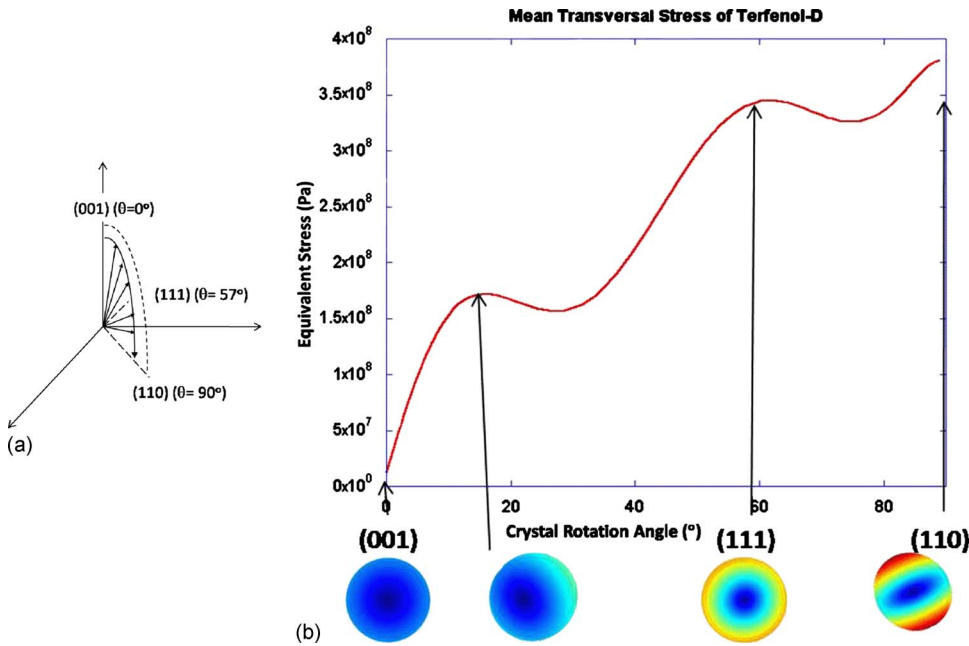


FIG. 5. (Color online) (a) Thickness direction of terfenol-D aligned from crystallographic (001) to (111) to (110) direction. (b) Mean transversal stress of terfenol-D corresponds to the crystal rotation.

a 17% improvement in ME coefficient can be obtained by aligning the  $\langle 110 \rangle$  crystallographic direction of terfenol-D along the applied magnetic field direction. In addition, when terfenol-D is aligned along  $\langle 110 \rangle$  crystallographic direction,

stress in radial direction is not uniform. This leads to a possibility of future improvement of ME coefficient by engineering the shape of composite system.

## ACKNOWLEDGMENTS

This work has been supported by the National Science Foundation under Grant No. DMR-0407462. Partial work was reported by Jimmy H. Wang published by the thesis office, the Pennsylvania State University.

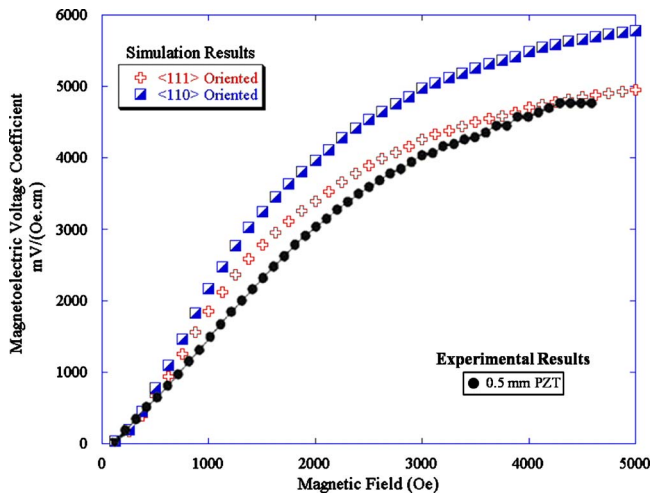


FIG. 6. (Color online) ME voltage coefficients vs magnetic field plot of experimental data, simulated results for  $\langle 111 \rangle$  oriented terfenol-D and  $\langle 110 \rangle$  oriented terfenol-D direction.

- <sup>1</sup>W. F. Brown, R. M. Hornreic, and S. Shtrikman, *Phys Rev.* **168**, 574 (1968).
- <sup>2</sup>W. Roentgen, *Annu. Rev. Phys. Chem.* **35**, 586 (1888).
- <sup>3</sup>P. Curie, *J. Phys.: Conf. Ser.* **3**, 393 (1894).
- <sup>4</sup>I. E. Dzyaloshinskii, *Zh. Eksp. Teor. Fiz.* **37**, 881 (1959).
- <sup>5</sup>E. Ascher, H. Rieder, H. Schmid, and H. Stossel, *J. Appl. Phys.* **37**, 1404 (1966).
- <sup>6</sup>J. Ryu, S. Priya, K. Uchino, and H. Kim, *J. Electroceram.* **8**, 107 (2002).
- <sup>7</sup>S. Priya, R. Islam, S. Dong, and D. Viehland, *J. Electroceram.* **19**, 147 (2007).
- <sup>8</sup>R. E. Newnham, *Properties of Materials: Anisotropy, Symmetry, Structure*, 1st ed. (Oxford University Press, Oxford, 2005).
- <sup>9</sup>L. Sandlund, M. Fahlander, T. Cedell, A. E. Clark, J. B. Restorff, and M. Wun-Fogle, *J. Appl. Phys.* **75**, 5656 (1994).
- <sup>10</sup>J. H. Wang, R. Guo, and A. S. Bhalla, *Ferroelectr., Lett. Sect.* **34**, 46 (2007).
- <sup>11</sup>P. Langevin, *J. Phys. (France)* **4**, 678 (1905).